Chapter 16
Undesirable Anisotropy in a Discrete Fiber Bundle Model of Fibrous Tissues

Cormac Flynn and M.B. Rubin

Abstract Lanir (J Biomech. 16(1):1–12, 1983) proposed a structural model for the anisotropic response of fibrous tissues with fiber bundles oriented in space by a continuous orientation distribution. Each fiber bundle was assumed to have the same undulation distribution that characterizes its nonlinear elastic response. Recently, a discrete fiber icosahedron model for fibrous soft tissues has been introduced, which is based on fiber bundles parallel to the six lines that connect opposing vertices of a regular icosahedron. Although the parameters in the icosahedron model can be determined to match experimental data for the anisotropic response of various tissues, the icosahedron model predicts anisotropic response when the weights of the six fiber bundles are equal. This chapter quantifies this undesirable anisotropic response and refers to a new icosahedron model based on a generalized invariant which also matches experimental data and analytically reduces to an isotropic form when the weights of the fiber bundles are equal.

16.1 Introduction

Lanir (1983) proposed a structural model for the anisotropic elastic response of fibrous tissues which was based on the idea that the tissue is a collection of fiber bundles that are characterized by continuous orientation and undulation distribution functions. More specifically, it was assumed that each fiber bundle is a collection of coiled or undulated fibers and that an individual fiber does not resist compression or extension when it is undulated. Consequently, it resists extension only when it is straight. Thus, the undulation distribution characterizes the nonlinear response of

C. Flynn (✉)
Centre for Engineering and Industrial Design, Wintec-Waikato Institute of Technology, Tristram St, Whitiora, Hamilton 3200, New Zealand
e-mail: Cormac.Flynn@wintec.ac.nz

M.B. Rubin
Faculty of Mechanical Engineering, Technion—Israel Institute of Technology, Haifa 32000, Israel
e-mail: mbrubin@tx.technion.ac.il

G.S. Kassab, M.S. Sacks (eds.), *Structure-Based Mechanics of Tissues and Organs*,
DOI 10.1007/978-1-4899-7630-7_16

the fiber bundle to stretching. Moreover, it was assumed that undulation distribution is independent of orientation with each fiber bundle exhibiting the same response to extension.

Within the context of this type of structural model the strain energy function is expressed as a double integral over the orientation and undulation distributions. Due to nonlinearity induced by general undulation distributions, it is usually not possible to evaluate these integrals analytically. A number of procedures for numerical integration over a sphere have been discussed in Bazant and Oh (1986), Ehret et al. (2010), and Itskov et al. (2010) which evaluate the integrand at a finite set of specific orientations and which cause varying degrees of unphysical anisotropy due to discretization.

Structural models with a finite collection of fibers have been used to study the response of low-density materials with open cells and fiber-dominated matrix composites (Christensen 1986; Christensen 1987). Models of this type that are based on orientations determined by opposing vertices of a regular icosahedron and of a dodecahedron (ten fibers) have been studied in Elata and Rubin (1994, 1995). Also, an icosahedron model for anisotropic response of fibrous soft tissue using six discrete fiber bundles oriented in the directions of opposing vertices of a regular icosahedron was recently considered in Flynn et al. (2011). Specifically, in Flynn et al. (2011) the strain energy function for each fiber bundle was assumed to be the same function of the stretch of the fiber bundle and the strain energy of the entire tissue was taken to be a weighted sum of the strain energies of each of the six fiber bundles in the discrete icosahedron model. Moreover, the strain energy function was determined by simple undulation distributions which ensure that the fiber bundle cannot be compressed. It was shown in Flynn et al. (2011) that the weights and the material parameters of the undulation distribution can be determined to match large deformation experimental data for the anisotropic response of various tissues. However, it was also noted in Flynn et al. (2011) that for the proposed undulation distributions, the tissue response was not isotropic even when the weights of the strain energy of each fiber bundle are the same. This means that unequal weights cannot be interpreted as the sole contribution to anisotropy.

The objective of this chapter is to analyze this undesirable anisotropy induced by fiber undulation distributions in a discrete icosahedron model similar to the one discussed in Flynn et al. (2011). An outline of this chapter is as follows. Section 16.2 describes a simplified icosahedron model for which the strain energy function of each fiber bundle is taken to be a function of the Lagrangian strain of the fiber bundle and not its stretch. As in Flynn et al. (2011), the strain energy of the entire tissue is a weighted sum of the strain energies of the specified fiber bundles. Section 16.3 uses the response to isochoric extension to quantify undesirable anisotropy caused by the nonlinearity of simple undulation distributions. The undesirable anisotropy caused by discreteness of the icosahedron model is also analyzed in Sect. 16.4 using a refined icosahedron model for which the strain energy function is an average of the strain energy function for N icosahedron models with different fiber orientations. Section 16.5 introduces a randomly oriented fiber model and Sect. 16.6 presents conclusions.

16.2 An Icosahedron Model of the Fiber Distribution

For an icosahedron model of the fiber distribution the six unit vectors $\mathbf{N}_i$ ($i = 1$, 2, ..., 6) that are parallel to the six lines connecting opposing vertices of a regular icosahedron are specified relative to the rectangular Cartesian base vectors $\mathbf{e}_i$ ($i = 1$, 2, 3) by the expressions (see Fig. 16.1)

$$\begin{aligned}
\mathbf{N}_1 &= \frac{2}{\sqrt{5}}\mathbf{e}_1 + \frac{1}{\sqrt{5}}\mathbf{e}_3, \mathbf{N}_2 = \frac{1}{2}\left(1 - \frac{1}{\sqrt{5}}\right)\mathbf{e}_1 + \sqrt{\frac{1}{2}\left(1 + \frac{1}{\sqrt{5}}\right)}\ \mathbf{e}_2 + \frac{1}{\sqrt{5}}\mathbf{e}_3, \\
\mathbf{N}_3 &= -\frac{1}{2}\left(1 + \frac{1}{\sqrt{5}}\right)\mathbf{e}_1 + \sqrt{\frac{1}{2}\left(1 - \frac{1}{\sqrt{5}}\right)}\ \mathbf{e}_2 + \frac{1}{\sqrt{5}}\mathbf{e}_3, \\
\mathbf{N}_4 &= -\frac{1}{2}\left(1 + \frac{1}{\sqrt{5}}\right)\mathbf{e}_1 - \sqrt{\frac{1}{2}\left(1 - \frac{1}{\sqrt{5}}\right)}\ \mathbf{e}_2 + \frac{1}{\sqrt{5}}\mathbf{e}_3, \\
\mathbf{N}_5 &= \frac{1}{2}\left(1 - \frac{1}{\sqrt{5}}\right)\mathbf{e}_1 - \sqrt{\frac{1}{2}\left(1 + \frac{1}{\sqrt{5}}\right)}\ \mathbf{e}_2 + \frac{1}{\sqrt{5}}\mathbf{e}_3, \quad \mathbf{N}_6 = \mathbf{e}_3.
\end{aligned} \tag{16.1}$$

Moreover, it is convenient to define the symmetric structural tensors $\mathbf{B}_i$, such that

$$\mathbf{B}_i = \mathbf{N}_i \otimes \mathbf{N}_i \,(\text{no sum on } i = 1, 2, \ldots, 6)\,, \tag{16.2}$$

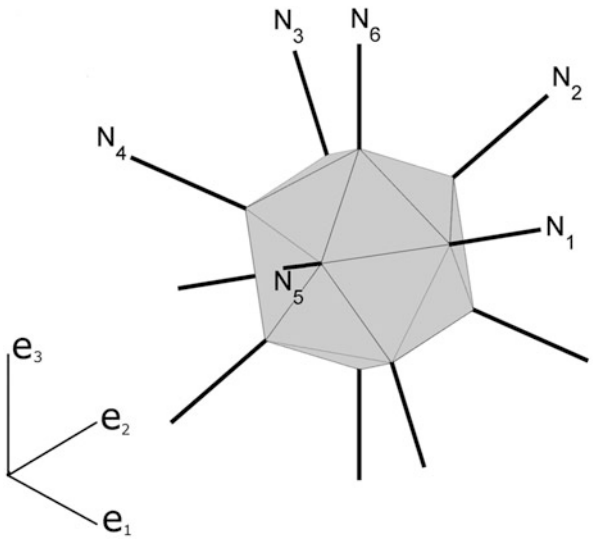

Fig. 16.1 Sketch of a regular icosahedron showing the vectors $\mathbf{N}_i$

where $\bigotimes$ denotes the tensor product operator. Then, using the work in Elata and Rubin (1994) it can be shown that for an arbitrary second order tensor $\mathbf{E}$

$$\sum_{i=1}^{6} \mathbf{B}_i = 2\,\mathbf{I}, \quad \sum_{i=1}^{6} \mathbf{B}_i \cdot \mathbf{E} = 2\,\mathbf{E} \cdot \mathbf{I}, \tag{16.3a, b}$$

$$\sum_{i=1}^{6} (\mathbf{B}_i \otimes \mathbf{B}_i) \cdot (\mathbf{E} \otimes \mathbf{E}) = \sum_{i=1}^{6} (\mathbf{B}_i \cdot \mathbf{E})^2 = \frac{2}{5}\left[(\mathbf{E} \cdot \mathbf{I})^2 + 2\,(\mathbf{E} \cdot \mathbf{E})\right], \tag{16.3c}$$

where $\mathbf{I}$ is the second order unity tensor, $\mathbf{A} \cdot \mathbf{B} = \text{tr}\left(\mathbf{A}\mathbf{B}^{\text{T}}\right)$ denotes the inner product between two second order tensors $\{\mathbf{A}, \mathbf{B}\}$ and (16.3c) generalizes the inner product operator for fourth order tensors.

Next, recall that a material point located by $\mathbf{X}$ in the reference configuration is deformed to the position $\mathbf{x}$ in the present configuration at time t. The mapping from the reference to present configurations, the deformation gradient $\mathbf{F}$, dilatation J, and Lagrangian strain $\mathbf{E}$ are given by

$$\mathbf{x} = \mathbf{x}\,(\mathbf{X},\ t)\,, \quad \mathbf{F} = \partial\mathbf{x}/\partial\mathbf{X}, \quad J = \det(\mathbf{F}) > 0, \quad \mathbf{E} = \frac{1}{2}\,(\mathbf{C} - \mathbf{I})\,, \quad \mathbf{C} = \mathbf{F}^{\text{T}}\mathbf{F}. \tag{16.4}$$

Moreover, the Lagrangian strains E_i $(i = 1, 2, \ldots, 6)$ of the material fibers in the $\mathbf{N}_i$ directions are defined by

$$E_i = \mathbf{E} \cdot \mathbf{B}_i\,(i = 1,\ 2, \ldots,\ 6)\,. \tag{16.5}$$

Now, for a compressible hyperelastic material the strain energy function W per unit mass for the icosahedron model is specified by

$$\rho_0 W = \sum_{i=1}^{6} w_i f\,(E_i), \quad w_i \geq 0, \quad \sum_{i=1}^{6} w_i = 1, \tag{16.6}$$

where ρ_0 is the reference mass density, the strain energy function f of each fiber bundle has the same form, and w_i are nonnegative weighting functions. Using the usual arguments it follows that the symmetric Piola–Kirchhoff stress $\mathbf{S}$ and the Cauchy stress $\mathbf{T}$ associated with (16.6) are given by

$$\mathbf{S} = \sum_{i=1}^{6} w_i \frac{df\,(E_i)}{dE_i}\mathbf{B}_i, \quad \mathbf{T} = J^{-1}\mathbf{F}\mathbf{S}\mathbf{F}^{\text{T}}. \tag{16.7a, b}$$

For the simple case of a single fiber bundle it follows that

$$w_1 = 1 \quad \text{all other} \quad w_i = 0, \quad S_1 = \mathbf{S} \cdot \mathbf{B}_1 = \frac{df\,(E_1)}{dE_1}, \tag{16.8}$$

so that the stiffness K of the fiber bundle is given by

$$K = \frac{dS_1}{dE_1} = \frac{d^2 f\,(E_1)}{dE_1^2}. \tag{16.9}$$

As discussed by Lanir (1983), the collagen fiber bundles in soft connective tissues are typically coiled in the stress-free reference configuration and the stress response of each fiber bundle is characterized by an undulation distribution $D(x)$ which is normalized so that

$$\int_0^\infty D(x)\ dx = 1, \tag{16.10}$$

where the fraction of fibers that are straight at the strain E is given by

$$\int_0^E D(x)\ dx. \tag{16.11}$$

Furthermore, assuming that the stiffness of each collagen fiber in the bundle is constant E_c when the fiber is straight, the function f in (16.9) is determined by integrating the expression

$$\frac{d^2 f(E)}{dE^2} = E_c \int_0^E D(x)\ dx \quad \text{for} \quad E \geq 0. \tag{16.12}$$

In this expression it is tacitly assumed that the fiber in the bundle is coiled when it is compressed and that it makes no contribution to the stress when it is not straight ($E \leq 0$).

To investigate undesirable anisotropy caused by nonlinearity of the undulation distribution in the discrete icosahedron model, the weights are taken to be equal

$$w_i = \frac{1}{6}\,(i = 1,\ 2, \ldots,\ 6)\,, \tag{16.13}$$

and the strain energy function of the tissue is given by

$$\rho_0 W = \frac{1}{6}\sum_{i=1}^{6} f\,(E_i). \tag{16.14}$$

16.2.1 Anisotropic Response Case I

The simplest distribution considered in Flynn et al. (2011) is a step distribution that vanishes for $x \leq x_1$ and $x > x_2$ and is constant in the interval $x_1 \leq x \leq x_2$, such that

$$\begin{aligned} D(x) &= 0 \qquad \text{for } x < x_1 \ \text{ and } \ x > x_2, \\ D(x) &= \frac{1}{x_2 - x_1} \text{for } 0 \leq x_1 \leq x \leq x_2, \end{aligned} \tag{16.15}$$

where x_1 is a nonnegative constant that characterizes the strain when the first fiber in the fiber bundle becomes straight. It then follows that the solution $f_{\rm I}$ of (16.12) is given by

$$\begin{aligned} f(E) = f_{\rm I}(E) &= \frac{E_{\rm c}\langle E - x_1\rangle^3}{6\,(x_2 - x_1)} && \text{for } E \le x_2, \\ f(E) = f_{\rm I}(E) &= \frac{E_{\rm c}(x_2 - x_1)^2}{6} + \frac{E_{\rm c}\,(E - x_1)\;\,(E - x_2)}{2} && \text{for } E > x_2, \end{aligned} \tag{16.16}$$

where the Macaulay brackets $\langle x\rangle$ are defined by

$$\langle x\rangle = \frac{1}{2}\,(x + |x|)\,. \tag{16.17}$$

16.2.2 Isotropic Response

For the simple case when the stiffness of the collagen fiber bundle is constant $E_{\rm c}$ and the fiber is allowed to resist compression, the strain energy function f in (16.9) is given by

$$f(E) = \frac{E_{\rm c}E^2}{2}. \tag{16.18}$$

It follows from (16.3c), (16.5), and (16.14) that the associated strain energy function for the tissue is an isotropic function of the strain $\mathbf{E}$ given by

$$\rho_0 W = \frac{E_{\rm c}}{12}\sum_{\rm i=1}^{6} E_i^2 = \frac{E_{\rm c}}{30}\Big[(\mathbf{E}\cdot\mathbf{I})^2 + 2\,(\mathbf{E}\cdot\mathbf{E})\Big]. \tag{16.19}$$

16.2.3 Anisotropic Response Case II

In order to analyze the influence of the assumption that the fibers cannot support compression when they are coiled, the strain energy function (16.19) is modified to take the form

$$f(E) = f_{\rm II}(E) = \frac{E_{\rm c}}{2}\langle E - x_1\rangle^2, \quad \rho_0 W = \frac{E_{\rm c}}{12}\sum_{i=1}^{6}\langle E_i - x_1\rangle^2. \tag{16.20}$$

Figure 16.2 plots the functions $f_{\rm I}$ and $f_{\rm II}$ that characterize the strain energy of the fiber bundles associated with (16.16 and 16.20), respectively.

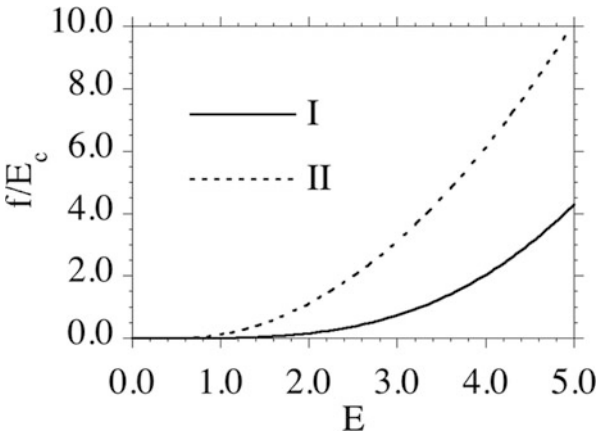

Fig. 16.2 Functions f_{I} and f_{II} characterizing the strain energy of fiber bundles

16.3 An Example of Isochoric Extension

In order to prove that a strain energy function characterizes isotropic response it is necessary to prove analytically that it depends on the strain $\mathbf{E}$ only through its invariants. In contrast, it is sufficient to consider a single numerical simulation to prove that a strain energy function exhibits undesirable anisotropy. To this end, it is convenient to define the right-handed orthonormal triad $\mathbf{a}_i$ in the reference configuration with $\{\mathbf{a}_1, \mathbf{a}_2\}$ being in the plane of the vectors $\{\mathbf{N}_1, \mathbf{N}_2 + \mathbf{N}_6\}$, such that

$$\mathbf{a}_1 = \mathbf{N}_1, \quad \mathbf{a}_2 = \mathbf{a}_3 \times \mathbf{a}_1, \quad \mathbf{a}_3 = \frac{\mathbf{a}_1 \times (\mathbf{N}_2 + \mathbf{N}_6)}{|\mathbf{a}_1 \times (\mathbf{N}_2 + \mathbf{N}_6)|}. \tag{16.21}$$

Moreover, it can be shown that the angle β between $\mathbf{a}_1$ and the vector $(\mathbf{N}_2 + \mathbf{N}_6)$ is given by

$$\beta = \cos^{-1}\left(\frac{\sqrt{2}}{\sqrt{5+\sqrt{5}}}\right) > 0. \tag{16.22}$$

Then, it is possible to define another right-handed orthonormal triad of vectors $\mathbf{A}_i$ parametrically in terms of the parameter α, such that

$$\begin{gathered}\mathbf{A}_1 = \cos(\alpha\beta)\ \mathbf{a}_1 + \sin(\alpha\beta)\ \mathbf{a}_2,\ \mathbf{A}_2 = -\sin(\alpha\beta)\ \mathbf{a}_1 + \cos(\alpha\beta)\ \mathbf{a}_2, \\ \mathbf{A}_3 = \mathbf{a}_3, \qquad\qquad 0 \le \alpha < 1.\end{gathered} \tag{16.23}$$

Specifically, this causes $\mathbf{A}_1$ to rotate about the $\mathbf{A}_3$ axis from the orientation $\mathbf{a}_1$ to the vector $\mathbf{a}_2$ that is parallel to $(\mathbf{N}_2 + \mathbf{N}_6)$ as α ranges from zero to unity (see Fig. 16.3).

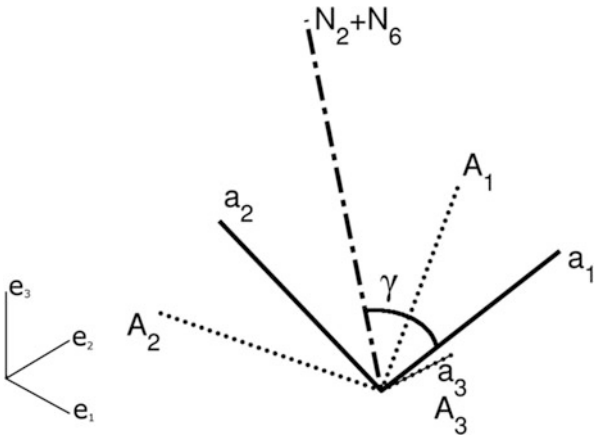

Fig. 16.3 Sketch of the angle γ and triads $\mathbf{a}_i$ and $\mathbf{A}_i$ of vectors characterizing the orientation of the sample of material that is being loaded in isochoric extension

Next, consider isochoric extension relative to $\mathbf{A}_i$ and specify $\mathbf{F}$ in the form

$$\mathbf{F} = a\,\mathbf{A}_1 \otimes \mathbf{A}_1 + \frac{1}{\sqrt{a}}\left(\mathbf{A}_2 \otimes \mathbf{A}_2 + \mathbf{A}_3 \otimes \mathbf{A}_3\right), \quad a > 0, \tag{16.24}$$

where a is the stretch of a material fiber in the $\mathbf{A}_1$ direction. It follows that this deformation field can be used to examine the response of samples of the material with different orientations in the reference configuration (characterized by the value of α) to the same isochoric extension (characterized by the value of a).

Using the deformation (16.24), it is possible to calculate the value of the strain energy as a function of $\{a, \alpha\}$. In particular, when the weights w_i are equal (16.13), the strain energy function (16.14) takes the values $\{W_{\mathrm{I}}, W_{\mathrm{II}}\}$, respectively, for the specifications (16.16) and (16.20) with

$$\rho_0 W_{\mathrm{I}}(a,\alpha) = \frac{1}{6}\sum_{i=1}^{6} f_{\mathrm{I}}(E_i), \quad \rho_0 W_{\mathrm{II}}(a,\alpha) = \frac{1}{6}\sum_{i=1}^{6} f_{\mathrm{II}}(E_i). \tag{16.25}$$

Therefore, the relative errors $\{ER_{\mathrm{I}}, ER_{\mathrm{II}}\}$ in these strain energy functions for a specific value of a and varying values of α can be defined by

$$ER_{\mathrm{I}}(\alpha) = \frac{W_{\mathrm{I}}(a,\alpha)}{W_{\mathrm{I}}(a,0)} - 1, \quad ER_{\mathrm{II}}(\alpha) = \frac{W_{\mathrm{II}}(a,\alpha)}{W_{\mathrm{II}}(a,0)} - 1. \tag{16.26a, b}$$

In the following example it will be shown that both of the models (16.16 and 16.20) predict undesirable anisotropy even though the weights w_i have been taken to be equal (16.13). Specifically, for the example specify

$$x_1 = 1, \quad x_2 = 4, \quad a = 3. \tag{16.27}$$

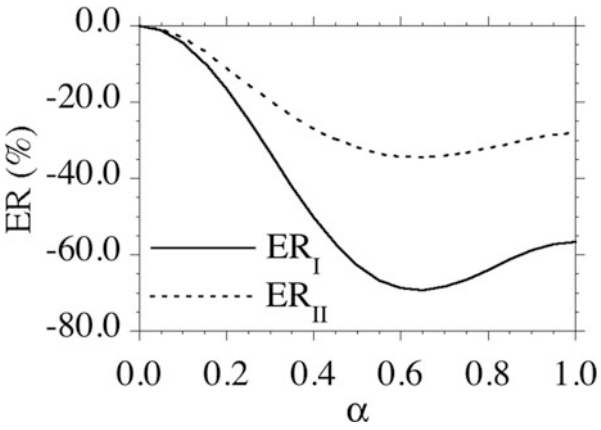

Fig. 16.4 Errors $\{ER_{\rm I}, ER_{\rm II}\}$ quantifying the undesirable anisotropy for the two icosahedron models characterized by the undulation distributions, (16.16) and (16.20), respectively

Figure 16.4 plots the errors $\{ER_{\rm I}, ER_{\rm II}\}$ as functions of α. The maximum magnitudes of these errors are about $\{69\,\%, 34\,\%\}$, respectively, for $\{ER_{\rm I}, ER_{\rm II}\}$. Since the values of these errors are nonzero, it follows that nonlinearity of the undulation distribution causes undesirable anisotropy in the discrete icosahedron model. Moreover, comparison of (16.16) with the isotropic strain energy (16.18) indicates that anisotropy predicted by (16.16) {i.e., $ER_{\rm I}$} is due to both the cubic dependence on strain and the presence of the cutoff strain $E = x_1$. In contrast, comparison of (16.20) with the isotropic strain energy (16.18) indicates that anisotropy predicted by (16.20) {i.e., $ER_{\rm II}$} is due solely to the cutoff strain $E = x_1$.

16.4 A Refined Icosahedron Model

In order to further analyze the influence of discreteness of the icosahedron model on undesirable anisotropy, it is convenient to define a refined icosahedron model. Within the context of the icosahedron model described in Sect. 16.2, it is necessary to evaluate the strain energy function for only six directions defined by the vectors $\mathbf{N}_i$ in (16.1). A refined icosahedron model can be obtained by defining the strain energy function as an average of $N = 6\{5(4)^{J-1} + 1\}$ icosahedron models with N structural tensors $\mathbf{B}_i$ associated with N fiber orientations. The value of J $(=1, 2\ \ldots)$ determines the level of refinement as discussed presently.

To this end, it is noted that vectors $\mathbf{N}_i$ in (16.1) can be used to define five equilateral triangles with the following triads of vectors locating the vertices of the triangles

$$\{\mathbf{N}_I,\ \mathbf{N}_{I+1},\ \mathbf{N}_6\}\ \text{for}\ I = 1,\ 2, \ldots,\ 4, \quad \{\mathbf{N}_5,\ \mathbf{N}_1,\ \mathbf{N}_6\}\ \text{for}\ \ I = 5, \tag{16.28}$$

each of which has the same vertex located by $\mathbf{N}_6$. These five triangles can be tessellated into 4^{J-1} equilateral triangles $(J = 1,\ 2, \ldots)$ as shown in Fig. 16.5.

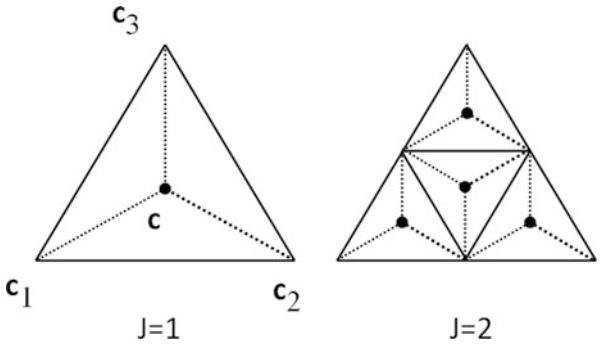

Fig. 16.5 Sketch of tessellation of an equilateral triangle into 4^{J-1} equilateral triangles

For example, a typical triangle has vertices located by the three unit vectors $\mathbf{c}_i$ ($i = 1$, 2, 3) and its centroid is located by the unit vectors $\mathbf{c}$ defined by

$$\mathbf{c} = \frac{\mathbf{c}_1 + \mathbf{c}_2 + \mathbf{c}_3}{|\mathbf{c}_1 + \mathbf{c}_2 + \mathbf{c}_3|}. \tag{16.29}$$

Next, the proper orthogonal rotation tensor $\mathbf{R}(\mathbf{c})$ is defined which rotates the vector $\mathbf{N}_6$ to the vector $\mathbf{c}$ counterclockwise by the angle δ about the unit direction $\mathbf{n}_3$, which is normal to the $\mathbf{N}_6$–$\mathbf{c}$ plane. Specifically, define the right-handed triad of vectors $\mathbf{n}_i$ by the expressions

$$\mathbf{n}_1 = \mathbf{N}_6, \quad \mathbf{n}_2 = \frac{\mathbf{c} - (\mathbf{c}\cdot\mathbf{n}_1)\,\mathbf{n}_1}{|\mathbf{c} - (\mathbf{c}\cdot\mathbf{n}_1)\,\mathbf{n}_1|}, \quad \mathbf{n}_3 = \mathbf{n}_1 \times \mathbf{n}_2. \tag{16.30}$$

Then, $\mathbf{R}(\mathbf{c})$ can be written in the form

$$\mathbf{R}\,(\mathbf{c}) = (\cos\delta\mathbf{n}_1 + \sin\delta\mathbf{n}_2) \otimes \mathbf{n}_1 + (-\sin\delta\mathbf{n}_1 + \cos\delta\mathbf{n}_2) \otimes \mathbf{n}_2 + \mathbf{n}_3 \otimes \mathbf{n}_3, \tag{16.31}$$

where the acute angle δ between the vectors $\mathbf{n}_1 = \mathbf{N}_6$ and $\mathbf{c}$ is given by

$$\delta = \cos^{-1}(\mathbf{n}_1 \cdot \mathbf{c})\,. \tag{16.32}$$

For each value of $\mathbf{R}(\mathbf{c})$ an additional icosahedron model is generated using the six structural tensors $\mathbf{B}_i$ ($i = 1, 2, \ldots, 6$) in (16.2) to obtain the following six additional structural tensors

$$\mathbf{R}(\quad)\mathbf{R}^{\mathrm{T}}(\mathbf{c}) \quad \text{for } i = 1,\ 2, \ldots,\ 6. \tag{16.33}$$

The resulting refined model has N structural tensors $\mathbf{B}_i$, associated with N fiber orientations and the strain energy function is specified by

$$\rho_0 W = \rho_0 W_1\,(a,\ \alpha) = \frac{1}{N}\sum_{i=1}^{N} f_1\,(E_i), \quad E_i = \mathbf{E}\cdot\mathbf{B}_i \quad (i = 1,\ 2, \ldots,\ N)\,. \tag{16.34}$$

In these expressions, E_i is the component of the Lagrangian strain of a fiber bundle in the direction $\mathbf{B}_i$, the function f_{I} associated with the undulation distribution of the fiber bundle is specified by (16.16), and the parameters $\{\alpha, a\}$ in (16.23) and (16.24) characterize the loading. This model has N fibers, which are equally weighted. In this regard, it should be emphasized that the definitions of the fiber orientations in the refined icosahedron model are different conceptually from orientations used to obtain numerical approximations of integrals over the unit sphere, which are weighted unequally in order to increase accuracy of integrating specific functional forms (e.g., Ehret et al. 2010; Bazant and Oh 1985). Moreover, it is noted that since $\mathbf{B}_i$ ($i = 1, 2, \ldots, 6$) satisfy (16.3a) it follows that the refined icosahedron model has the symmetry that

$$\sum_{i=1}^{N} \mathbf{B}_i = \frac{3}{N}\mathbf{I}, \tag{16.35}$$

for any level of refinement J.

As an example, use is made of the specifications (16.27) and the error ER_{I} is defined by (16.6). Figure 16.6 shows predictions of the error ER_{I} for different values of refinement. Specifically, for $N = 6$ the results correspond to the simple icosahedron model described in Sect. 16.2; and the other predictions correspond to the refined icosahedron model with $N = 36$ for $J = 1$, $N = 126$ for $J = 2$, and $N = 486$ for $J = 3$. Also, Fig. 16.7 focuses attention on the results for the higher values of N. These results indicate that even for a relatively simple strain energy function a large number of fibers are needed to obtain nearly isotropic material response. At this point it is not clear why the error predicted by the refined icosahedron model does not reduce monotonically with increased refinement.

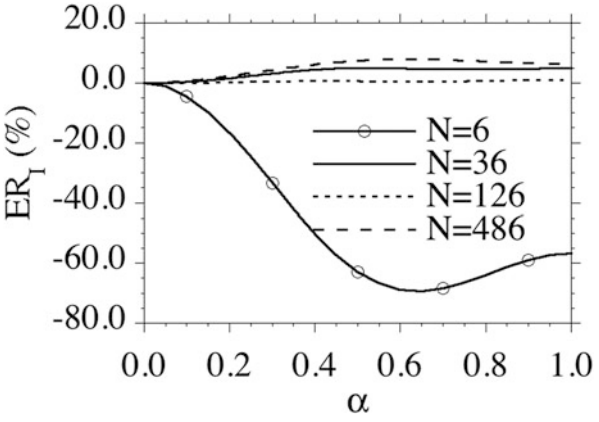

Fig. 16.6 Reduction in the error ER_{I} predicted by the refined icosahedron model for the values $N = 6$, 36, 126, 486 of the number of fiber bundles in the model

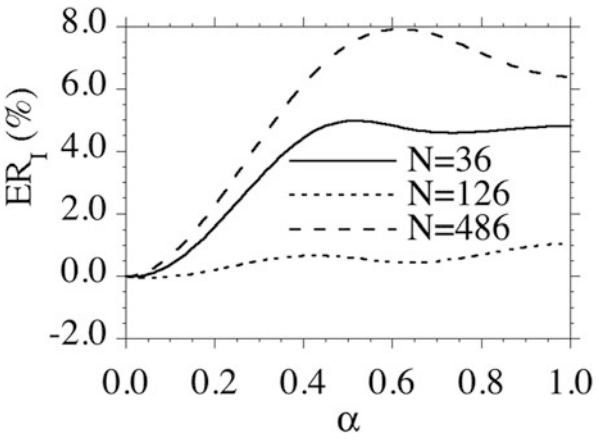

Fig. 16.7 Reduction in the error ER_{I} predicted by the refined icosahedron model for the higher values $N = 36$, 126, 486 of the number of fiber bundles in the model

16.5 Equal Area Model

It is well known that the regular polyhedron (Platonic solid) with the greatest number of faces is the regular icosahedron with 20 faces. Consequently, with regard to numerical integration schemes over the unit sphere, Bazant and Oh (1985) state that "we cannot have, for a hemisphere, a numerical integration formula with more than $N = 10$ regularly spaced points ...." Nevertheless, in this section it is of interest to consider a model based on N oriented fibers which locate the centroids of patches of a hemisphere that have equal areas. In particular, this model is used in conjunction with the refined icosahedron model of the Sect. 16.4 to help quantify the number of fibers needed to reduce the error due to unphysical anisotropy.

An approximate uniform distribution of fibers can be developed by dividing the surface area of a hemisphere into patches that have the same areas. Specifically, consider the unit vector $\mathbf{N}$ defined in terms of the spherical polar angles $\{\theta, \phi\}$ by

$$\mathbf{N} = \mathbf{N}(\theta,\ \phi) = \sin(\phi)\left[\cos(\theta)\,\mathbf{e}_1 + \sin(\theta)\,\mathbf{e}_2\right] + \cos(\phi)\,\mathbf{e}_3. \tag{16.36}$$

It follows that the upper surface of hemisphere is characterized by the ranges

$$0 \le \theta \le 2\pi, \quad 0 \le \cos(\phi) \le 1. \tag{16.37}$$

Moreover, the area A of a patch on a hemisphere with unit radius for $\{\theta, \phi\}$ in the ranges $\Theta_i \le \theta \le \Theta_{i+1}$ and $\Phi_j \le \phi \le \Phi_{j+1}$ is given by

$$A = (\Theta_{i+1} - \Theta_i)\ \left[\cos\left(\Phi_j\right) - \cos\left(\Phi_{j+1}\right)\right]. \tag{16.38}$$

Consequently, the area of this hemisphere can be divided into $N = K^2$ equal areas by specifying $\{\Theta_i, \Phi_j\}$ in the forms

$$\Theta_i = \frac{2\pi\,(i-1)}{K} \quad \text{for } i = 1,\ 2,\ \ldots,\ K+1,$$
$$\Phi_j = \cos^{-1}\left(\frac{K+1-j}{K}\right) \quad \text{for } j = 1,\ 2,\ \ldots,\ K+1. \tag{16.39}$$

Then, the values $\{\theta_i, \phi_j\}$ of $\{\theta, \phi\}$, which locate the centroids of these regions can be defined by

$$\theta_i = \frac{1}{2}\left(\Theta_i + \Theta_{i+1}\right) \quad \text{for } i = 1,\ 2,\ \ldots,\ K,$$
$$\phi_j = \cos^{-1}\left[\frac{1}{2}\left\{\cos\left(\Phi_j\right) + \cos\left(\Phi_{j+1}\right)\right\}\right] \quad \text{for } j = 1,\ 2,\ \ldots,\ K. \tag{16.40}$$

Now, using these values $\{\theta_i, \phi_j\}$ the fibers are oriented in the N directions $\mathbf{N}_i$ defined by (16.36) with θ taking the K values θ_i for each of the K values of ϕ_j. Also, the associated structural tensors $\mathbf{B}_i$ are given by

$$\mathbf{B}_i = \mathbf{N}_i \otimes \mathbf{N}_i \,(\text{no sum on } i = 1,\ 2,\ \ldots,\ N)\,. \tag{16.41}$$

Next, it is convenient to define the average structural tensor $\overline{\mathbf{B}}$ by the expression

$$\overline{\mathbf{B}} = \frac{1}{N}\sum_{i=1}^{N} \mathbf{B}_i. \tag{16.42}$$

For fibers uniformly distributed over the hemisphere, it would be expected that this average structural tensor would be a scalar times the unity tensor $\mathbf{I}$. Consequently, an error measure of uniformity can be defined in terms of the relative magnitude of the deviatoric part $\overline{\mathbf{B}}'$ of $\overline{\mathbf{B}}$ defined by

$$ER_{\mathrm{B}} = \sqrt{\frac{9\overline{\mathbf{B}}' \cdot \overline{\mathbf{B}}'}{\left(\overline{\mathbf{B}} \cdot \mathbf{I}\right)^2}}, \quad \overline{\mathbf{B}}' = \overline{\mathbf{B}} - \frac{1}{3}\left(\overline{\mathbf{B}} \cdot \mathbf{I}\right)\mathbf{I} \tag{16.43}$$

Due to the result (16.35), the refined icosahedron model will predict that ER_{B} vanishes for all levels of refinement.

For the equal area model the strain energy function $W_{\mathrm{I}}(a, \alpha)$ is specified by (16.34) and the error $ER_{\mathrm{I}}(\alpha)$ is specified by (16.26a) using the values (16.27) and the deformation (16.24). Figure 16.8 shows the predictions of $ER_{\mathrm{I}}(\alpha)$ for different values of the number N of fibers and Table 16.1 records the associated values of the error ER_{B} in (16.43). These results indicate that for $N = 49$ the equal area model is less accurate than the refined icosahedron model for $N = 36$. However, the monotonic error reduction with increasing values of N predicted by the equal area model suggests that the fibers are more uniformly distributed in the model than

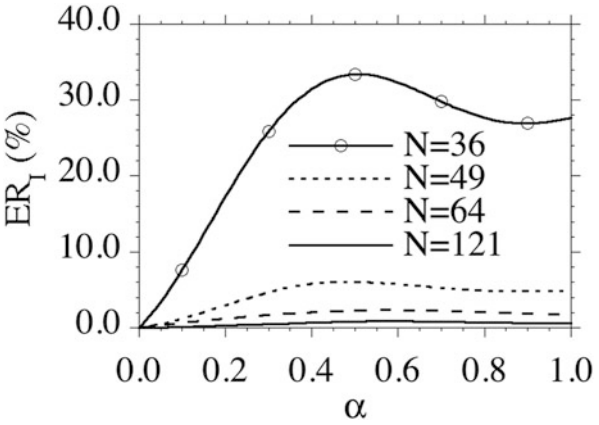

Fig. 16.8 Reduction in the error ER_{I} predicted by the equal area model for different values of the number N of fibers

Table 16.1 Values of the error ER_{B} in (16.40) predicted by the equal area model

N	ER_{B} (%)
36	0.85
49	0.62
64	0.48
121	0.25

in the refined icosahedron model. Moreover, it is noted that the equal area model predicts the error due to unphysical anisotropy to be less than 3 % for $N = 64$. Even for this simple strain energy function, the computational effort required to evaluate the equal area model for $N = 64$ is significant since the constitutive equation must be evaluated at each Gauss point in a finite element program. An alternative model that significantly reduces the computational effort is discussed in the next section.

16.6 Conclusions

The structural model for anisotropic elastic response of fibrous connective tissue proposed by Lanir (1983) has the simplicity that the undulation distribution of fibers in each fiber bundle is independent of the orientation distribution. This suggests that the orientation distribution can be correlated to histological observations of fiber orientations. In particular, a random orientation of fibers should lead to isotropic response of the tissue. However, from a computational point of view it is necessary to discretize the evaluation of the integral over the orientation region. This discretization yields a finite number N of nonlinear strain energy functions (characterizing fiber bundles in specified orientations) that need to be evaluated for each strain at each material point.

The example in Sect. 16.4 considered a refined icosahedron model and the example in Sect. 16.5 considered an equal area model. For each of these models

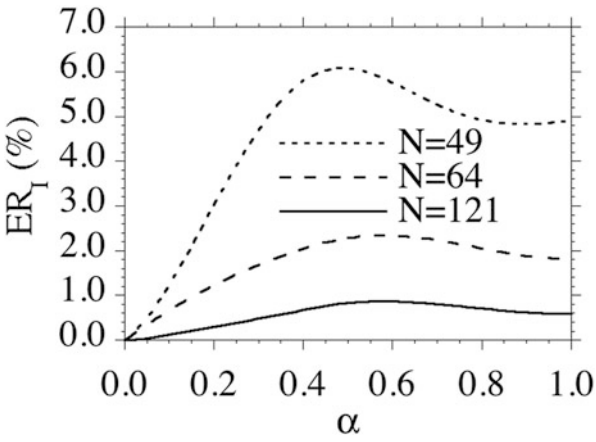

Fig. 16.9 Reduction in the error ER_{I} predicted by the equal area model for the higher values $N = 49, 64, 121$ of the number of fiber bundles in the model

the strain energy function needs to be evaluated for each of the N fibers. Also, the Cauchy stress is expressed in terms of a weighted sum of N symmetric tensors $\mathbf{B}_{\mathrm{i}}$ defined in (16.33). It was shown in Figs. 16.7 and 16.9 that the error ER_{I} due to unphysical anisotropy for the refined icosahedron model is less than 5 % for $N = 36$ and for the uniform area model is less than 7 % for $N = 49$. Of course, the magnitude of the unphysical anisotropy depends on the specific loadings considered. Moreover, these levels of refinement cause considerable increased complexity, which may not be justified by the accuracy and availability of experimental data.

Within the context of the icosahedron model proposed in Flynn et al. (2011) the tissue is modeled by only six fiber bundles, each of which has the same undulation distribution. This model can be thought of as a specific discretization of the model in Lanir (1983). It was shown in Flynn et al. (2011) that this icosahedron model can successfully reproduce experimental data exhibiting anisotropic response. However, it was shown in Sect. 16.3 here that this icosahedron model exhibits significant undesirable anisotropy when the weighting functions w_i in (16.6) are equal (16.13). This means that anisotropy in the model is influenced by both the nonlinearity of the undulation distribution and differences in the values of the weights. Consequently, the weights w_i are not pure measures of anisotropy of the histological orientations of fibers in the tissue.

Itskov and Ehret (2009) have proposed an alternative model of tissues which is based on a generalized invariant of deformation determined by a weighted average of different structural tensors. This idea has been used in Flynn and Rubin (2012) to develop a generalized icosahedron model. Specifically, a generalized structural tensor $\mathbf{W}$ is defined in terms of the weights w_i and the structural tensors $\mathbf{B}_i$ in (16.2) of the icosahedron model by

$$\mathbf{W} = \sum_{i=1}^{6} w_i \ \mathbf{B}_i, \quad w_i \geq 0, \quad \mathbf{W} \cdot \mathbf{I} = \sum_{i=1}^{6} w_i = 1. \tag{16.44}$$

Also, the generalized strain invariant γ is defined by

$$\gamma = \left(\mathbf{C} + \mathbf{C}^{-1}\right) \cdot \mathbf{W} - 2 \geq 0, \tag{16.45}$$

where $\mathbf{C}$ is the right Cauchy–Green deformation tensor (16.4). Then, the strain energy is taken to be a nonlinear function of γ. In view of the property (16.3a) of $\mathbf{B}_i$ it follows that for equal weights w_i (16.13), γ becomes an isotropic invariant of $\mathbf{C}$ given by

$$\gamma = \frac{1}{3}\left(\mathbf{C} + \mathbf{C}^{-1}\right) \cdot \mathbf{I} - 2 \geq 0. \tag{16.46}$$

In particular, the response of the tissue is analytically isotropic for any nonlinear dependence of the strain energy on γ in (16.46). Moreover, it was shown in Flynn and Rubin (2012) that when the strain energy is a simple polynomial function of γ, the coefficients of the polynomial and the weights w_i can be determined to match large deformation experimental data for the anisotropic response of various tissues.

The advantages of this generalized icosahedron model are that the number of material constants is small, it can be simplified to produce isotropic response exactly and γ depends on only a single structural tensor $\mathbf{W}$ so the constitutive response is simple to evaluate numerically. Specifically, this is a phenomenological model that characterizes a coupled network of fiber bundles. In this regard, the generalized icosahedron model has the disadvantage that the nonlinear elastic response of the model is not simply connected to an undulation distribution of each fiber bundle, as proposed in the structural model of Lanir (1983).

Acknowledgments This research was partially supported by MB Rubin's Gerard Swope Chair in Mechanics. The authors would also like to acknowledge helpful discussions with A Rubin about the equal area model.

References

Bazant Z, Oh BH. Microplane model for progressive fracture of concrete and rock. J Eng Mech ASCE. 1985;111(4):559–82.

Bazant ZP, Oh BH. Efficient numerical integration on the surface of a sphere. Z Angew Math Mech. 1986;66(1):37–49.

Christensen RM. Mechanics of low density materials. J Mech Phys Solids. 1986;34(6):563–78.

Christensen RM. Sufficient symmetry conditions for isotropy of the elastic moduli tensor. J Appl Mech. 1987;54(4):772–7.

Ehret AE, Itskov M, Schmid H. Numerical integration on the sphere and its effect on the material symmetry of constitutive equations—a comparative study. Int J Numer Methods Eng. 2010;81(2):189–206.

Elata D, Rubin MB. Isotropy of strain energy functions which depend only on a finite number of directional strain measures. J Appl Mech. 1994;61(2):284–9.

Elata D, Rubin MB. A new representation for the strain energy of anisotropic elastic materials with application to damage evolution in brittle materials. Mech Mater. 1995;19(2–3):171–92.

Flynn C, Rubin MB. An anisotropic discrete fibre model based on a generalised strain invariant with application to soft biological tissues. Int J Eng Sci. 2012;60:66–76.

Flynn C, Rubin MB, Nielsen P. A model for the anisotropic response of fibrous soft tissues using six discrete fibre bundles. Int J Numer Methods Biomed Eng. 2011;27(11):1793–811.

Itskov M, Ehret AE. A universal model for the elastic, inelastic and active behaviour of soft biological tissues. GAMM-Mitteilungen. 2009;32(2):221–36.

Itskov M, Ehret AE, Dargazany R. A full-network rubber elasticity model based on analytical integration. Math Mech Solids. 2010;15:655–71.

Lanir Y. Constitutive equations for fibrous connective tissues. J Biomech. 1983;16(1):1–12.